Bioelectromagnetics 24:262–276 (2003)

Radio Frequency Electromagnetic Field Exposure in Humans: Estimation of SAR Distribution in the Brain, Effects on Sleep and Heart Rate

Reto Huber,[1] Jürgen Schuderer,[2] Thomas Graf,[1] Kathrin Jütz,[1] Alexander A Borbély,[1] Niels Kuster,[3] and Peter Achermann[1]*

[1]*Institute of Pharmacology and Toxicology, University of Zürich, Zürich, Switzerland*
[2]*Integrated Systems Laboratory, ETH Zürich, Zürich, Switzerland*
[3]*Foundation for Research on Information Technologies in Society (IT'IS),VAW/ETHZ, Zürich, Switzerland*

In two previous studies we demonstrated that radiofrequency electromagnetic fields (RF EMF) similar to those emitted by digital radiotelephone handsets affect brain physiology of healthy young subjects exposed to RF EMF (900 MHz; spatial peak specific absorption rate [SAR] 1 W/kg) either during sleep or during the waking period preceding sleep. In the first experiment, subjects were exposed intermittently during an 8 h nighttime sleep episode and in the second experiment, unilaterally for 30 min prior to a 3 h daytime sleep episode. Here we report an extended analysis of the two studies as well as the detailed dosimetry of the brain areas, including the assessment of the exposure variability and uncertainties. The latter enabled a more in depth analysis and discussion of the findings. Compared to the control condition with sham exposure, spectral power of the non-rapid eye movement sleep electroencephalogram (EEG) was initially increased in the 9–14 Hz range in both experiments. No topographical differences with respect to the effect of RF EMF exposure were observed in the two experiments. Even unilateral exposure during waking induced a similar effect in both hemispheres. Exposure during sleep reduced waking after sleep onset and affected heart rate variability. Exposure prior to sleep reduced heart rate during waking and stage 1 sleep. The lack of asymmetries in the effects on sleep EEG, independent of bi- or unilateral exposure of the cortex, may indicate involvement of subcortical bilateral projections to the cortex in the generation of brain function changes, especially since the exposure of the thalamus was similar in both experiments (approx. 0.1 W/kg). Bioelectromagnetics 24:262–276, 2003.

Key words: global system for mobile communications (GSM); mobile phones; nonREM sleep; electroencephalogram; spectral analysis; heart rate variability

INTRODUCTION

The present approach focuses on the investigation of radiofrequency electromagnetic fields (RF EMF) effects of two different specific absorption rate (SAR) distributions on sleep electroencephalogram (EEG) and heart rate. The EEG is the principal state indicator of sleep. Slow waves (0.75–4.5 Hz) and sleep spindles (12–15 Hz), the two salient features of non-rapid eye movement (nonREM) sleep, can be quantified and used as markers of sleep regulating processes. In recent years it has become increasingly evident that these typical oscillations in the EEG are closely associated with cellular changes at the level of thalamic and cortical neurons [Steriade et al., 1993, 1994; McCormick and Bal, 1997]. Sleep is an endogenous, self-sustained cerebral process, and the sleep EEG is well characterized,

Grant sponsor: Swiss National Science Foundation; Grant number: 3100-053005.97; Grant sponsor: Human Frontiers Science Program; Grant numbers: RG-81/96, RG-0131/2000; Grant sponsors: Swisscom; Swiss Federal Office of Public Health (Experiment 2); Research Cooperation Sustainable Mobile Communications (simulation of SAR distribution).

*Correspondence to: Dr. Peter Achermann, Ph.D., Institute of Pharmacology and Toxicology, University of Zürich, Winterthurerstrasse 190, Zürich CH-8057, Switzerland.
E-mail: acherman@pharma.unizh.ch

Received for review 8 April 2002; Final revision received 3 December 2002

DOI 10.1002/bem.10103
Published online in Wiley InterScience (www.interscience.wiley.com).

so that even minor physiological or pharmacological effects can be recognized. This has been shown for hormonal changes during the menstrual cycle [Driver et al., 1996] and pregnancy [Brunner et al., 1994], as well as for residual effects of hypnotics [Borbély et al., 1983, 1985] and stimulants [Landolt et al., 1995a,b]. Even two types of insulin, which differ only in a single amino acid, have been discriminated in diabetic patients based on their sleep EEG [Roth et al., 1998].

Several studies investigating the effects of RF EMF exposure on human sleep have been previously carried out. Mann and Röschke [1996] reported a reduction of REM sleep and changes in spectral power of the EEG during REM sleep. In two follow up studies, no effects from RF EMF on sleep and sleep EEG were found [Wagner et al., 1998, 2000]. In contrast, we reported that exposure to RF EMF either during sleep [Borbély et al., 1999] or during waking prior to sleep [Huber et al., 2000] affected the nonREM sleep EEG. In the latter studies, the field conditions were well defined and the dosimetry was thoroughly evaluated.

Effects from RF EMF exposure on cognitive functions have been investigated by several groups. RF EMF exposure speeded up response times in simple reaction time, vigilance and working memory tasks [Preece et al., 1999; Koivisto et al., 2000a,b]. In a working memory task, event-related desynchronization and synchronization of the waking EEG showed increased power in the 8–10 Hz [Krause et al., 2000b] and in the 6–8 and 8–10 Hz [Krause et al., 2000c] frequency ranges during RF EMF exposure. The authors hypothesized that RF EMF exposure modulates the response of EEG oscillatory activity around 8 Hz specifically during cognitive processing [Krause et al., 2000a]. In a recent study in narcoleptics, effects of RF EMF exposure on visual event-related potentials were observed and reaction times were reduced [Jech et al., 2001].

Effects of RF EMF exposure on heart rate are contradictory [Braune et al., 1998, 2002]. Heart rate variability has also been found to be affected by low frequency electromagnetic fields [Sastre et al., 1998, 2000]. These findings may not transfer to RF EMF.

The aim of the present report is an extended analysis of the effects of RF EMF exposure with two different distributions [Borbély et al., 1999; Huber et al., 2000] of the SAR on EEG topography (different derivations) and on heart rate and heart rate variability. An important aspect of this report is the dosimetry. The two studies differ not only in the timing of exposure with respect to sleep but also with respect to the induced field distribution within the brain. In order to quantify those differences in SAR upon functional brain regions, a detailed FDTD analysis with a novel, 23 tissue type, anatomical head model was performed. Only a detailed and extensive dosimetry enables a differential and in depth analysis and discussion of the experimental findings.

MATERIALS AND METHODS

Design of Experiments 1 and 2

Subjects and data recording

Experiment 1. In Expt 1 [for details see Borbély et al., 1999], nocturnal sleep of 24 healthy, young, right handed men was recorded during a night with exposure to RF EMF and a night with sham exposure (no RF EMF). The experiment consisted of two sessions of two consecutive nights at an interval of one week. In each session, an experimental night was preceded by a pre-experimental night. During exposure nights, RF EMF was turned on and off intermittently at 15 min intervals, starting with the on condition at lights off. The pre-experimental night was recorded in a room different from the experimental night.

The electroencephalogram (EEG derivations: F3, C3, P3, O1, F4, C4, P4, O2, referenced to Cz and C3A2), the submental electromyogram [chin EMG; Rechtschaffen and Kales, 1968], the electrooculogram (EOG, differential recording), and the electrocardiogram (EKG) were continuously recorded with a polygraphic amplifier [for signal conditioning and sampling see Borbély et al., 1999]. For the EKG, consecutive RR intervals (time interval between consecutive R waves) and heart rate per 20 s (beats per minute, as calculated from the mean RR interval) were stored. An R wave was detected whenever the rectified first derivative of the EKG exceeded approximately 40% of the maximum. All variables were recorded during the entire sleep episode.

Electromagnetic interference with the recording equipment was eliminated by placing the amplifiers within two metallic boxes and using fedthrough π filters for all input and output connections in order to block any RF coupling to the leads.

In Expt 1, in addition to the electrophysiological recordings, simultaneous time lapse, all night video recordings of the subject's torso were obtained.

Experiment 2. Sixteen healthy, young, right handed men participated in Expt 2 [for details see Huber et al., 2000]. One of them was also a subject in Expt 1. The subjects were exposed to RF EMF for 30 min prior to a 3 h morning sleep episode. The time between the end of exposure and lights off was 10 min. To ensure a continuous daytime sleep episode, sleep in the preceding night was restricted to 4 h. Subjects remained in the lab

and were under constant supervision between the two sleep episodes. The experiment consisted of three sessions separated by one week intervals. The three sessions involved right hemispheric exposure, left hemispheric exposure, and sham exposure.

The EEG (F3, C3, P3, O1, F4, C4, P4, O2, Cz, referenced to linked mastoids), EMG, EOG, and EKG were continuously recorded [for signal conditioning and sampling see Huber et al., 2000]. During exposure prior to sleep waking data were also recorded. To minimize eye movement artifacts during the first, middle, and last three minutes of the wake EEG recordings, subjects were requested to fixate upon a black dot on the wall. The EKG was analyzed as in Expt 1. Recording equipment was shielded as in Expt 1.

At the end of the experiment subjects were asked to assign the experimental condition for each experimental day.

Data analysis and statistics

Sleep stages and EEG analysis. Sleep stages were visually scored for 20 s epochs according to standard criteria [Rechtschaffen and Kales, 1968]. NonREM–REM sleep cycles were defined as in previous experiments [Aeschbach and Borbély, 1993]. Power spectra of consecutive 20 s epochs (FFT routine, Hanning window, averages of five 4 s epochs) were computed for referential derivations (referenced to A2 in Expt 1 and to linked mastoids in Expt 2). Artifacts were excluded by visual inspection and semiautomatically [for more details see Borbély et al., 1999; Huber et al., 2000]. Only 20 s epochs without artifacts were used for further analysis. In Expt 2 the power spectra of the 30 min intervals were normalized with respect to the average power of nonREM sleep in the entire 3 h sleep episode.

To investigate the occurrence of activity in the spindle frequency range, the EEG (C3A2 or C3 linked mastoids) was band pass filtered (12–15 Hz). The mean amplitude of the signal was computed by calculating the standard deviation (SD) of consecutive 0.5 s epochs. This procedure resulted in a new time series with data points at 0.5 s intervals. Subsequently, the new time series was smoothed, and power spectra of 64 s epochs (FFT, Hanning window, detrended with mean value of epoch, frequency resolution 0.015625 Hz) shifted by 20 s were calculated for the entire sleep episode. For methodological details see Achermann and Borbély [1997]. To obtain a measure for the periodicity of spindle incidence, the peak in the average spectrum of each subject was determined visually; identification of a peak was not always possible.

Movement during sleep. To investigate whether an unconscious perception of the electromagnetic fields was present, movements and position of the subjects during sleep was assessed (Expt 1). The sleeping position and its changes were visually scored using time lapse video recordings of 20 s epochs that were synchronized with the sleep stages. Head, body, and arm movements were discriminated. Head positions were defined as ''left'' when there was a nose angle to the left between 60 and 90°, as ''right'' when there was a nose angle of 60–90° to the right (nose up was 0°). Body position was defined as ''right'' or ''left'' when subjects laid on their right or left shoulder, respectively.

Heart rate. Heart rate of 20 s epochs was matched with the vigilance states and average values over specific time intervals (see below, Table 6) were compared. Twenty second epochs containing RR intervals of 200 ms or less were excluded. Heart rate variability was assessed by spectral analysis of RR interval tachograms (length of RR interval vs. number of progressive beats) [Anonymous, 1996]. Determination of the RR intervals is described above. Power spectra (FFT routine, Hanning window) of 256 consecutive RR intervals (approximately 256 s; frequency resolution approximately 0.004 Hz) were calculated to investigate changes in the EKG. The frequency resolution was scaled according to the duration of the mean RR interval.

Statistical methods. To assess data from Expt 1, a two way, within subjects ANOVA was used with the repeated measures ''condition'' (sham or field exposure) and ''sequence'' (first night sham or field). In Expt 2, a two way, within subjects ANOVA was used with the repeated measures ''condition'' (sham, left or right hemisphere exposure) and ''sequence'' (sham exposure in the first, second, or third session). Where appropriate, contrasts were assessed by post hoc two-tailed paired *t*-tests. For most variables only significant contrasts are reported. Analysis of specific EEG frequency bands was performed to reduce the amount of multiple testing.

Experimental Setups

Antenna configuration (Experiment 1). The objective of Expt 1 was to expose the heads of subjects as homogeneously as possible and as independently as possible from particular sleeping postures. This was achieved by an array of three half-wavelength dipole antennas mounted behind the head of the recumbent subject at a distance of 30 cm. This near field setup resulted in fairly uniform, well defined exposure conditions at the location of the subject's head. Absorber

walls were placed around the antennas and the bed in order to prevent field disturbance by reflections in the environment and to achieve sham conditions in the neighboring rooms (<-20 dB).

A schematic illustration of the setup is given in Figure 1a. Analysis of the videos recorded during the night with an infrared camera showed that the distance between the top of the subject's head and the antenna array varied between 30–45 cm and the angle of incidence from -45° to 45°.

Antenna configuration (Experiment 2). The objectives of Expt 2 were (1) unilateral exposure to test the hypothesis that asymmetric exposure results in asymmetric EEG responses and (2) exposure that mimicked the exposure of a handset, as well as (3) minimal variability of the exposure from subject to subject.

This was achieved using planar, rectangular patch antennas (Huber & Suhner SPA 920/65/9/0/V) mounted at both sides of the head (Fig. 1b). The position was optimized with respect to achieving SAR uniformity of the exposed hemisphere and producing a high average SAR ratio between the exposed and non-exposed sides of the brain. The best compromise was found at 115 ± 5 mm distance between antenna and head, with the center of the antenna at 42 ± 10 mm vertically above the ear canal, i.e., approximately one third of the distance between the ear canal and the top of the head. The average SAR value of the exposed side of the head was eight times higher than that of the unexposed side. Either the right antenna, the left antenna, or neither was excited in a double blind protocol. Input power was continuously measured to control the exposure conditions.

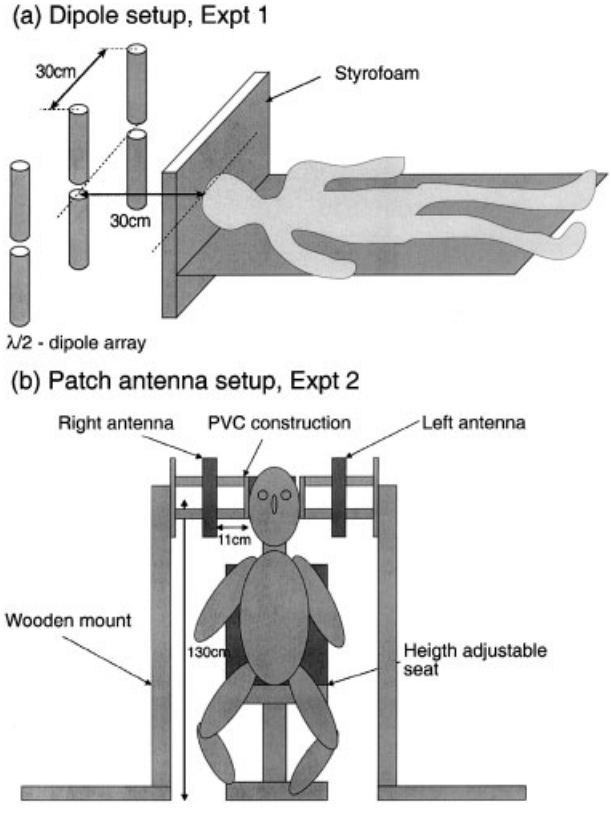

Fig. 1. Schematic diagrams of the exposure setups used in experiments 1 (Expt 1) and 2 (Expt 2).

Exposure signals (Experiments 1 and 2). The input power for each setup was adjusted to achieve the same 1 W/kg spatial peak SAR averaged over 10 g, which was determined according to the methodology defined for compliance testing of handsets [CENELEC, 2001]. The signal characteristics were also the same in both studies, corresponding to the synthesized base station-like GSM signal proposed for bioexperiments by Schüller et al. [2000]. Seven (slots 0–6) of the eight bursts (duration: 0.577 ms; intermittency between bursts: 20 μs) of the basic frame (4.61 ms) were on and one off (slot 7). Frames 26, 52, 78, and 104 of the multiframe (104 basic frame) were additionally modified: in addition to the 7th burst, the 1st burst was also idle for frames 26, 52, 78, and the 1st, 4th, and 7th bursts were idle for frame 104. This signal structure resulted in the spectral components of 2, 8, and 217 Hz, plus the corresponding harmonics. The burst and the intermittency between the bursts led to additional components at 1733 Hz and 50 kHz. The only difference in the signal characteristics was that in Expt 1 RF EMF was turned on and off intermittently at 15 min intervals. No standby mode transmission was applied during the 15 min off intervals.

Dosimetry

The detailed dosimetry, which provides SAR estimations for functional subregions inside the brain, was conducted by simulation. A series of measurements in free space and inside dielectric head phantoms were performed for verification purposes: (1) verification of the modeling of the antennas including the feeding source by measurements of the incident fields, and (2) verification of the simulated induced fields inside homogeneous phantoms. In addition, measurements were conducted to assess the effect of the electrodes on the induced fields (shielding/reflection and induced contact currents).

Computational tools and modeling. The simulation platform SEMCAD (Schmid & Partner Engineering AG, Zurich, Switzerland) was employed for this study. SEMCAD is based on the finite difference time domain (FDTD) method and is enhanced with unique features

for RF dosimetry, such as highly nestable subgrids and a special compound format enabling the handling of non homogeneous human models (www.semcad.com). The code has been broadly validated [e.g., Chavannes, 2002].

The dosimetry is based on the human head model derived from the data set of the head of a healthy female subject (age 40 years), consisting of 121 magnetic resonance images (MRI), with a slice separation of 1 mm in the ear region and 3 mm for the rest of the head [Burkhardt and Kuster, 2000]. For the purposes of this study, the precision of the discretization of the brain has been improved, and functional subregions have been derived from the original MRI slides. Table 1 shows the dielectric parameters of the 23 discriminated tissues, which were set according to the values given in Gabriel [1996]. For the quantification of left/right asymmetries of the SAR distribution in the head, the phantom was divided into two evaluation volumes. In order to enable maximum spatial resolution in the area of interest, an optimized graded mesh was used with a minimum voxel size of 1 mm^3 in the exposed head region, truncated by PML boundaries (total number of voxels approx. 15 million). The postprocessor of SEMCAD was extended to provide statistical data for each tissue type as well as for defined head areas (left side, right side, and entire head), e.g., mean SAR along with SD and 1 g averaged spatial peak SARs were computed.

The antenna units were modeled with voltage edge sources, and were harmonically excited at 900 MHz until a steady state was reached. For Expt 1, the three sources for the dipole antennas were placed between the dipole arms. The aperture coupled patch antenna in Expt 2 is excited via a microstrip feedline, whereby the edge source was located between the feedline and the metallic N plug holder.

Field mapping tool. For field measurements, the near field scanner DASY3 (Schmid & Partner Engineering AG, Zurich, Switzerland) was applied, equipped with the latest generation of free space and dosimetric probes (Table 2). DASY3 is the successor of the system described in [Schmid et al., 1996] and is based on a precisely controlled, 3 axis robotic arm, which can position all sorts of dosimetric probes. It allows highly sensitive field and temperature measurements in free space and inside phantoms. The verification of the appropriate modeling of the RF sources and the effect of the electrode leads on absorption and reflections were conducted with volunteers, the homogenous generic twin phantom [Kuster et al., 1997] and a homogeneous whole body phantom. The effect of the electrodes was analyzed in two ways: first, electrodes were fixed on the outside of the phantom shell and the SAR was measured inside tissue liquid. This method allows the assessment of the shielding effect of the electrode configuration, which results from reflections of the incident fields. Second, electrodes were taped along the inside of the phantom shell filled with head tissue-simulating liquid (tip of electrode in direct contact with liquid), in order to

TABLE 1. Dielectric Parameters of the Tissue Types Discriminated in the Human Head Model

Tissue type	ε_r[a]	σ [S/m][a]
Blood	61.4	1.54
Bone (cancellous)	20.8	0.34
Brain (grey matter)	52.7	0.94
Brain (white matter)	38.9	0.59
Cerebellum	49.4	1.26
Cerebro-spinal fluid	68.6	2.41
Cornea	55.2	1.39
Ear (avg. skin and cartilage)	42.0	0.82
Fat	5.5	0.05
Glands	59.7	1.04
Lenses	46.6	0.79
Lower jaw	20.8	0.34
Middle brain (grey matter)	52.7	0.94
Muscle	55.0	0.94
Skin	41.4	0.87
Skull	20.8	0.34
Spinal cord (grey matter)	52.7	0.94
Spine	20.8	0.34
Thalamus (grey matter)	52.7	0.94
Tongue	55.3	0.94
Upper jaw	20.8	0.34
Lateral ventricles	68.6	2.41
Vitreous humor	68.9	1.64
Generic phantom liquid	42.0	0.85

[a]Relative permittivity ε_r and the electric conductivity σ for the applied frequency of 900 MHz [Gabriel, 1996].

TABLE 2. Characteristics of the Free Space and Dosimetric Probes Used for Field Mapping

Probe type	Diameter [mm]	Dynamic range	Deviation of axial isotropy [dB]	Deviation of spherical isotropy [dB]
ET3DV6	6.8	2 mW/kg–100 W/kg	$<\pm0.05$	$<\pm0.20$
EF3DV2	3.9	2–1000 V/m	$<\pm0.05$	$<\pm0.30$
H3DV3	5.0	0.01–2 A/m	$<\pm0.05$	$<\pm0.20$

estimate local SAR increases, which could be caused by a coupling of induced RF currents on the electrodes and tissue.

RESULTS

Estimated Tissue SAR Values

Experiment 1. Dosimetry providing detailed information about the SAR distributions, variations, and uncertainties was conducted by utilizing the more sophisticated head model combined with the enhanced capability of the new simulation platform. The analysis confirmed the previous experimentally assessed ratio of spatial peak SAR with respect to the incident exposure.

Several posture conditions for the subjects with respect to the antenna array have been evaluated. Tissue models and SAR distributions corresponding to the aligned and 45° tilted head positions are shown in Figure 2. The 1 g averaged spatial peak SAR and the averaged SAR for the different brain tissues are summarized in Table 3. The values for ''brain average'' include the following brain tissues: white matter, grey matter, cerebellum, middle brain, thalamus, cerebrospinal fluid (CSF), and ventriculus lateralis. As expected, the exposure is symmetrical for all tissues with an untilted head position, i.e., head axis normal to the antenna array. The ratio between right and left hemispheres varies between 1.5–2 for the 45° tilted position, which represents the worst case asymmetrical configuration for Expt 1. The assessed mean SAR values, the variations and the uncertainty SD are given in Table 4.

All variation and uncertainties have been assessed according to NIST TN1297 [1994] and represent relative SD from the average value. The main parameters for variations in the exposure are: (1) changes in posture (head 45° tilted, head at 45 cm distance to dipoles, and head 25 cm horizontally displaced from the center dipole, which represents the largest variation); (2) changes of the electrode orientation relative to the incident fields due to subject movement; (3) different head sizes, assessed by scaling the human model by $\pm 10\%$, which was found to be the maximum variation in head size measured by Tisserand et al. [2001]; and (4) amplifier drifts. The parameters included in the uncertainty analysis of the dosimetry were the uncertainty from (1) the effect of electrodes, (2) probe calibrations, (3) dielectric parameters, and (4) the numerical model and discretization variation, assessed by comparing voxel sizes of 0.5, 1, and 3 mm^3.

Experiment 2. Modeling of the patch antenna had been validated based on far and near field experimental data [Christ et al., 1998]. Because of the close proximity to the head, the efficiency of the patch setup is about ten times higher than for the dipole setup, i.e., 0.54 W/kg per Watt antenna input power. Higher efficiency provides the advantage of enabling the application of signals with high crest factors, such as GSM basic (crest factor of 8.3) and DTX (crest factor of 69.3) with reasonable peak power requirements (crest factor = pulse peak power/average power). The results of the numerical analysis are shown in Table 3 and confirm that the SAR distributions in the exposed head side are comparable to those of Expt 1 and that a strong asymmetrical exposure had been achieved (Ratio column of Table 3). The position of the head with respect to the EM source can be kept very constant (variations of position $<\pm 5$ mm horizontally and $<\pm 30$ mm in the plane of the patch antenna). The variations and uncertainties were assessed according to the methodology defined above (Table 4).

Field Mapping

Experiment 1. The setup was initially analyzed in the dosimetric laboratory of ETH Zurich. The incident field distribution was first measured with a human volunteer lying on a bed with and without the presence of EEG electrodes attached to the head. Both conditions were compared with those of the homogeneous wholebody phantom ($\varepsilon_r = 42 \pm 2$ and $\sigma = 0.86 \pm 0.08$ S/m) placed at the same location. Similar disturbances of the incident field were observed. In the next step, the shielding effect of the electrodes was evaluated by fixing the electrodes at the outer shell of the phantom and by comparing the local SAR distributions of different orientations of the leads with respect to the incident field with the SAR distribution of the same setup without electrodes. Local variations of SAR were in the order of 40%.

Experiment 2. The numerical dosimetry was verified by replacing the non-homogenous phantom with the generic twin phantom filled with tissue simulating liquid ($\varepsilon_r = 41 \pm 2$ and $\sigma = 0.85 \pm 0.08$ S/m). This setup was experimentally and numerically analyzed, and area as well as spatial peak SAR values were compared. The deviation between measurement and simulation of less than 10% for the 1 and 10 g averaged spatial peak SAR confirmed the high quality of the numerical models.

The effect of the electrodes on the spatial peak SAR (shielding/reflection and wire induced currents) were evaluated as follows: the effect of shielding and disturbance of the source by reflections have been assessed by mounting all 15 electrodes at their position

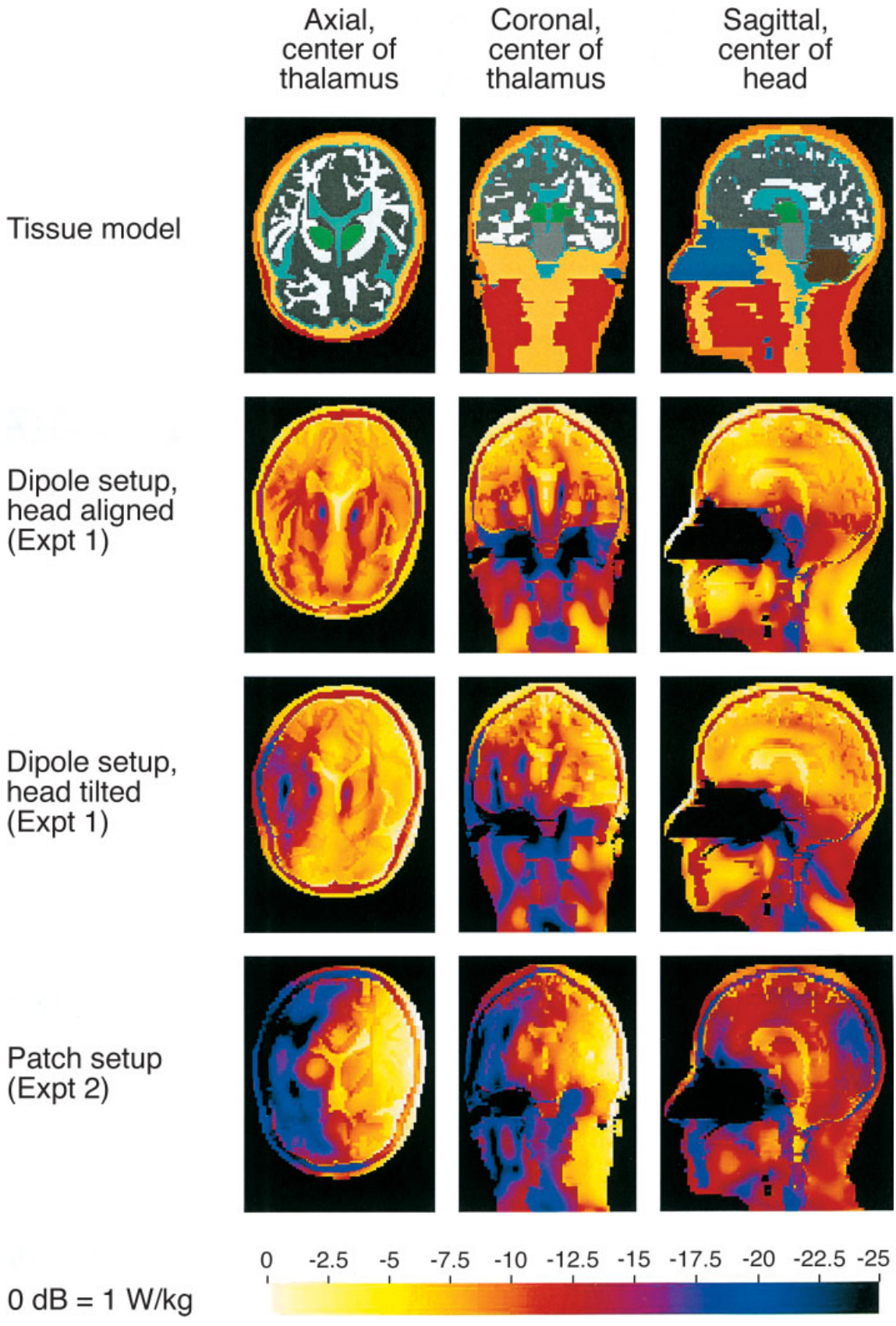
Axial, center of thalamus
Coronal, center of thalamus
Sagittal, center of head
Tissue model
Dipole setup, head aligned (Expt 1)
Dipole setup, head tilted (Expt 1)
Patch setup (Expt 2)
0 -2.5 -5 -7.5 -10 -12.5 -15 -17.5 -20 -22.5 -25
0 dB = 1 W/kg

Fig. 2.

TABLE 3. Computed Specific Absorbtion Rate (SAR, W/kg) of Head Tissues for the Dipole Setup Used in Expt 1 (Head Aligned and 45° Tilted to the Left) and for the Patch Antenna Setup Used in Expt 2

		Right hemisphere			Left hemisphere				Both hemispheres		
Tissue	Setup	1 g avg.[a]	Avg.[b]	SD[c]	1 g avg.	Avg.	SD	Ratio[d]	1 g avg.	Avg.	SD
Grey matter	Dip. aligned	0.43	0.18	0.09	0.45	0.18	0.09	1.02	0.45	0.18	0.09
	Dip. tilted	0.55	0.22	0.09	0.31	0.13	0.06	1.74	0.55	0.18	0.09
	Patch	1.02	0.25	0.19	0.15	0.03	0.03	7.90	1.02	0.15	0.18
White matter	Dip. aligned	0.26	0.11	0.05	0.25	0.12	0.05	0.94	0.26	0.12	0.05
	Dip. tilted	0.35	0.16	0.06	0.22	0.08	0.04	2.01	0.35	0.12	0.05
	Patch	0.61	0.20	0.13	0.08	0.02	0.01	10.7	0.61	0.10	0.12
Grey & white matter	Dip. aligned	0.40	0.17	0.08	0.45	0.16	0.08	1.03	0.45	0.16	0.08
	Dip. tilted	0.55	0.21	0.09	0.31	0.11	0.06	1.84	0.55	0.16	0.08
	Patch	0.97	0.24	0.18	0.14	0.03	0.02	8.65	0.97	0.13	0.16
Thalamus	Dip. aligned	0.19	0.11	0.07	0.12	0.08	0.04	1.42	0.19	0.10	0.06
	Dip. tilted	0.15	0.08	0.04	0.21	0.14	0.05	0.61	0.21	0.11	0.05
	Patch	0.16	0.13	0.02	0.13	0.10	0.03	1.36	0.16	0.12	0.03
Brain avg.	Dip. aligned	0.75	0.20	0.17	0.80	0.20	0.17	1.02	0.89	0.20	0.17
	Dip. tilted	0.77	0.24	0.17	0.57	0.14	0.12	1.66	0.77	0.19	0.15
	Patch	1.55	0.27	0.26	0.33	0.04	0.05	6.70	1.55	0.16	0.22
Brain avg. (without vent. lat.)	Dip. aligned	0.40	0.16	0.08	0.45	0.15	0.08	1.03	0.45	0.15	0.08
	Dip. tilted	0.55	0.19	0.09	0.31	0.11	0.06	1.81	0.55	0.15	0.08
	Patch	0.97	0.24	0.18	0.15	0.03	0.03	7.92	0.97	0.14	0.16

The brain-averaged values include grey matter, white matter, cerebellum, middle brain, thalamus, cerebro-spinal fluid (CSF) and lateral ventricles.
[a]Spatial peak SAR averaged over 1 g tissue.
[b]Average SAR over entire tissue.
[c]The SD of SAR inside the specific tissue.
[d]The ratio of the average SAR per tissue between the right and left hemispheres.

outside of the phantom shell. This configuration resulted in a reduction of 8 and 9% for the 1 and 10 g spatial peak SAR values, respectively. The effect of the wire induced currents was determined by fixing ear and eye electrodes at the inside of the shell (see Materials and Methods section, Dosimetry). A 35% higher 1 g but only 1% higher 10 g spatial peak SAR value was measured.

Sleep Stages

Experiment 1. Waking after sleep onset (WASO) was reduced after RF EMF exposure (Table 5; rANOVA, factors ''condition'' and ''sequence'' significant). Fifteen out of 24 subjects showed significantly less WASO after RF EMF exposure (values below upper limit of 95% confidence interval). The subgroup of 12 subjects who were first sham exposed exhibited overall larger reduction of WASO compared to the subgroup that was first field exposed. The number of subjects showing a significant decrease in WASO after RF EMF exposure was similar in both subgroups (7 and 8). The difference in WASO was due to a decrease in the mean duration of episodes of WASO (sham: 44.2 ± 6.4 s ($\pm$SEM); field: 33.2 ± 2.8 s; $P < .05$ two tailed paired t-test) rather than to a difference in the number of their occurrence (sham: 24.5 ± 2.4; field: 22.0 ± 1.5; n.s.). WASO did not differ in the pre-experimental nights between the two subgroups (first sham exposed; first field exposed). Therefore, the sequence effect cannot be explained by an intrinsic difference in WASO between the two subgroups.

None of the other sleep variables differed between the two conditions (Table 5).

Experiment 2. Sleep variables did not differ between RF EMF and sham exposure (Table 5).

REM sleep latencies were shorter compared to Expt 1 because of frequent sleep onset REM sleep episodes (i.e., occurrence of REM sleep within the first 15 min of sleep; in 9 subjects after sham exposure and left hemispheric exposure; in 10 subjects after right hemispheric exposure).

Fig. 2. Computed distribution of the specific absorption rate (SAR) for the tissue model shown in the top row: thalamus (green), grey matter (dark grey), white matter (white), CSF (cyan), cerebellum (brown), middle brain (light gray), muscle (dark orange), air (blue), skin (orange), and bone (yellow). The two middle rows show the SAR distributions for Expt 1 (head aligned and tilted 45° to the left) and the bottom row for Expt 2 (right antenna activated).

TABLE 4. Spatial and Time Averaged SAR Values (Expt 1 [Dipole Setup]: Entire Head Exposed, Expt 2 [Patch Setup]: Unihemispheric Exposure) and Estimation of the Variations and Uncertainties for the Dosimetric Assessment

Tissue	Setup[a]	Average SAR [W/kg]	Variation (%)	Dosimetric uncertainty (%)
Grey matter	Dipole	0.18	60	42
	Patch	0.25	19	15
White matter	Dipole	0.12	61	42
	Patch	0.20	17	15
Grey & white matter	Dipole	0.16	60	42
	Patch	0.24	19	15
Thalamus	Dipole	0.10	66	42
	Patch	0.13	29	15
Brain avg. (incl. vent.)	Dipole	0.20	60	42
	Patch	0.27	17	15
Brain avg. (without vent.)	Dipole	0.15	60	42
	Patch	0.24	17	15

[a]Average SAR values of both hemisperes (head aligned; Table 3) are given in case of the dipole setup and of the right hemisphere in case of the patch setup.

Sleep EEG

Experiment 1. An increase of nonREM sleep EEG power in the 11.5–12.25 and 13.5–14 Hz frequency bands was already present during the first 30 min interval after lights off, i.e., after 15 min of RF EMF exposure (Fig. 3). Because sleep latency was on average 11.2 min (Table 5), the effect is mainly seen during the first 15 min without field.

The topographical analysis is based on those frequency bands showing the largest change [Borbély et al., 1999]. Power in these bands was increased in most derivations (Fig. 4). The effect did not differ within and between hemispheres (two way repeated measure ANOVA with factors ''hemisphere'' (left or right) and ''derivation'' (frontal, central, parietal, occipital) performed with percentage increase, was not significant for the selected frequency bands).

To test for periodicities in the occurrence of sleep spindles, a new time series with data points at 0.5 s intervals was calculated. It was formed by the mean amplitude of the band-pass filtered EEG (12–15 Hz, see

TABLE 5. Effect of RF EMF Exposure on Sleep Variables Derived From Visual Scoring

	RF EMF exposure				
	Expt 1 [during sleep (n = 24)]		Expt 2 [prior to sleep (n = 16)]		
	Sham	Field	Sham	Left	Right
Time in bed	480.0	480.0	180.0	180.0	180.0
Total sleep time	445.9 (3.0)	451.2 (1.6)	163.1 (3.4)	167.4 (1.1)	164.7 (4.2)
Sleep latency	9.9 (1.6)	11.2 (1.6)	5.7 (0.9)	5.4 (1.1)	3.8 (1.1)
REM sleep latency	72.7 (5.0)	76.4 (5.6)	24.8 (8.1)	22.0 (6.9)	24.7 (7.0)
Waking after sleep onset (WASO)	18.2 (2.9)	12.1 (1.5)[a]	11.6 (3.7)	8.4 (1.1)	9.9 (3.3)
Stage 1	32.7 (2.3)	31.0 (2.6)	12.8 (2.0)	15.0 (2.7)	12.6 (1.8)
Stage 2	233.4 (5.1)	236.7 (5.4)	88.1 (6.2)	84.2 (6.2)	85.8 (4.9)
Stage 3	52.1 (2.1)	51.4 (2.6)	15.1 (2.9)	16.5 (2.7)	16.7 (2.6)
Stage 4	18.4 (2.9)	18.5 (3.3)	4.2 (1.7)	3.9 (1.7)	3.7 (1.6)
Slow-wave sleep	70.5 (4.4)	69.8 (4.6)	19.3 (4.3)	20.4 (3.5)	20.4 (3.6)
REM sleep	109.4 (3.3)	113.7 (3.5)	42.9 (4.4)	47.8 (3.3)	46.0 (3.6)
Movement time	5.6 (0.6)	5.2 (0.6)	3.4 (0.4)	3.0 (0.5)	3.1 (0.3)

Mean values (±SEM in parenthesis) in min are shown. Sleep onset was defined as first occurrence of stage 2, 3, 4, or REM sleep. Sleep latency, interval from lights off to sleep onset; REM sleep latency, interval from sleep onset to the first occurrence of REM sleep.
WASO: Two-way repeated measure ANOVA revealed significant effects for factors ''condition'' and ''sequence'' for exposure during sleep. Some of the sleep variables for exposure during sleep have been reported previously [Borbély et al., 1999], average data of left and right hemisphere exposure prior to sleep were presented in Huber et al. [2000].
[a]Significant difference to sham condition ($P < .05$, two tailed paired t-test).

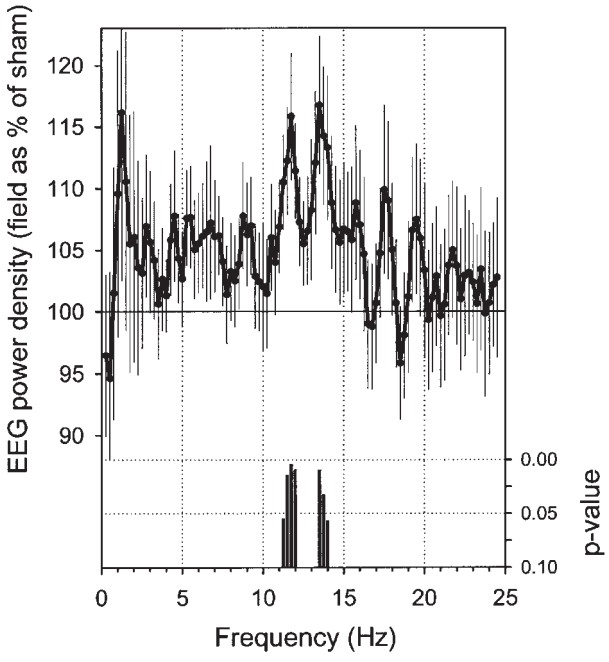

Fig. 3. Effect of RF EMF exposure on the nonREM sleep EEG during first 30 min after lights off, i.e., after 15 min of RF EMF exposure in Expt 1 (RF EMF exposure during sleep; n = 21 due to minimum criterion of 200 s nonREM sleep). Mean relative EEG power density spectrum (C3A2) in nonREM sleep is shown. The curve depicts power after field exposure (mean ± SEM for 0.25 Hz bins) expressed as a percentage of the corresponding value after sham exposure. Bars at the bottom indicate *P* values for frequency bins in which power was enhanced after RF EMF exposure (factor "condition" of two-way repeated measure ANOVA; "sequence" and interaction "condition" × "sequence" were not significant).

Materials and Methods section). Spindle frequency activity in nonREM sleep recurred at approximately 4 s intervals, which was reflected in a spectral peak at 0.22 Hz. The location of the spectral peaks did not differ between conditions (mean values for C3 in Hz ± SEM, n = 14, sham 0.22 ± 0.01; field 0.23 ± 0.01, $P > .2$, two tailed paired *t*-tests).

Experiment 2. The topographical analysis was performed using those frequency bands showing the largest change [Huber et al., 2000]. An increase of power was observed in most bands and derivations (Fig. 4). The effect did not differ within hemispheres and between left or right hemispheric exposure but was more pronounced in the left hemisphere for the 12.5–13.25 and 9–13.5 Hz bands irrespective of exposure side ($P < .05$, factor "hemisphere" (left, right), three-way repeated measure ANOVA, factors "condition" (left or right hemispheric exposure), "hemisphere," and "derivation" (frontal, central, parietal, occipital) performed with percentage increase).

Spindle frequency recurrence was reflected in a spectral peak at the following frequencies (for more details see Expt 1): sham 0.24 ± 0.01 Hz, n = 14; left exposure 0.22 ± 0.01 Hz, n = 15; right exposure 0.23 ± 0.01, n = 15; $P > .2$, two tailed paired *t*-tests.

Waking EEG

Experiment 1. Only a few frequency bins were affected in the waking EEG during exposure before sleep onset (increase of power in the 11–11.5 Hz range of waking and stage 1; derivation C3A2; n = 14, due to the minimum criterion of 100 s of artifact-free epochs).

Experiment 2. The average spectra of the waking EEG (derivation C3 against linked mastoids) of three 5 min episodes recorded during the 30 min RF EMF exposure (left or right hemisphere) showed a reduction of power compared to sham exposure in the 10.5–11 and 18.75–19.5 Hz frequency range ($P < .05$; two tailed paired *t*-test; minimum criterion of 100 s; n = 14 (left), n = 13 (right)).

Heart Rate and Heart Rate Variability

Experiment 1. Heart rate was not affected when subjects were exposed during sleep (Table 6). However, heart rate variability was affected. Spectral analysis of RR intervals revealed a 40.6 ± 7.3% decrease of power in the 0.10–0.11 Hz range ($P < .05$; 3 bins in low frequency range) after RF EMF exposure for the interval between lights off and sleep onset (only 8 subjects contributed to both conditions due to the minimum criterion of at least 512 RR intervals, approx. 8.5 min). After RF EMF exposure, mean spectra over the first three nonREM sleep episodes showed increased power in the 0.29–0.31 Hz range (5 bins, around peak in high frequency range, 54.8 ± 22.7% increase, $P < .05$). None of the all night mean spectra revealed differences between sham and field exposure.

Experiment 2. During the 30 min of RF EMF exposure no difference in heart rate between the three conditions was observed. Heart rate in waking and stage 1 of the entire sleep episode was reduced after exposure of the right and left hemispheres and before sleep onset after right hemisphere exposure (Table 6; no order effect). Heart rate variability (spectra of RR intervals) was altered during the 3 h sleep episode but not during the first half hour of nonREM sleep. Power in the 0.18–0.22 Hz frequency range (11 bins around peak in high frequency range, mean spectra of left and right hemisphere exposure) was increased by 47.4 ± 17.8% in the 3 h sleep episode after field exposure.

Sleep Posture (Experiment 1)

Under both conditions, subjects slept mainly on their back (body position back: 61.9 ± 3.9; side:

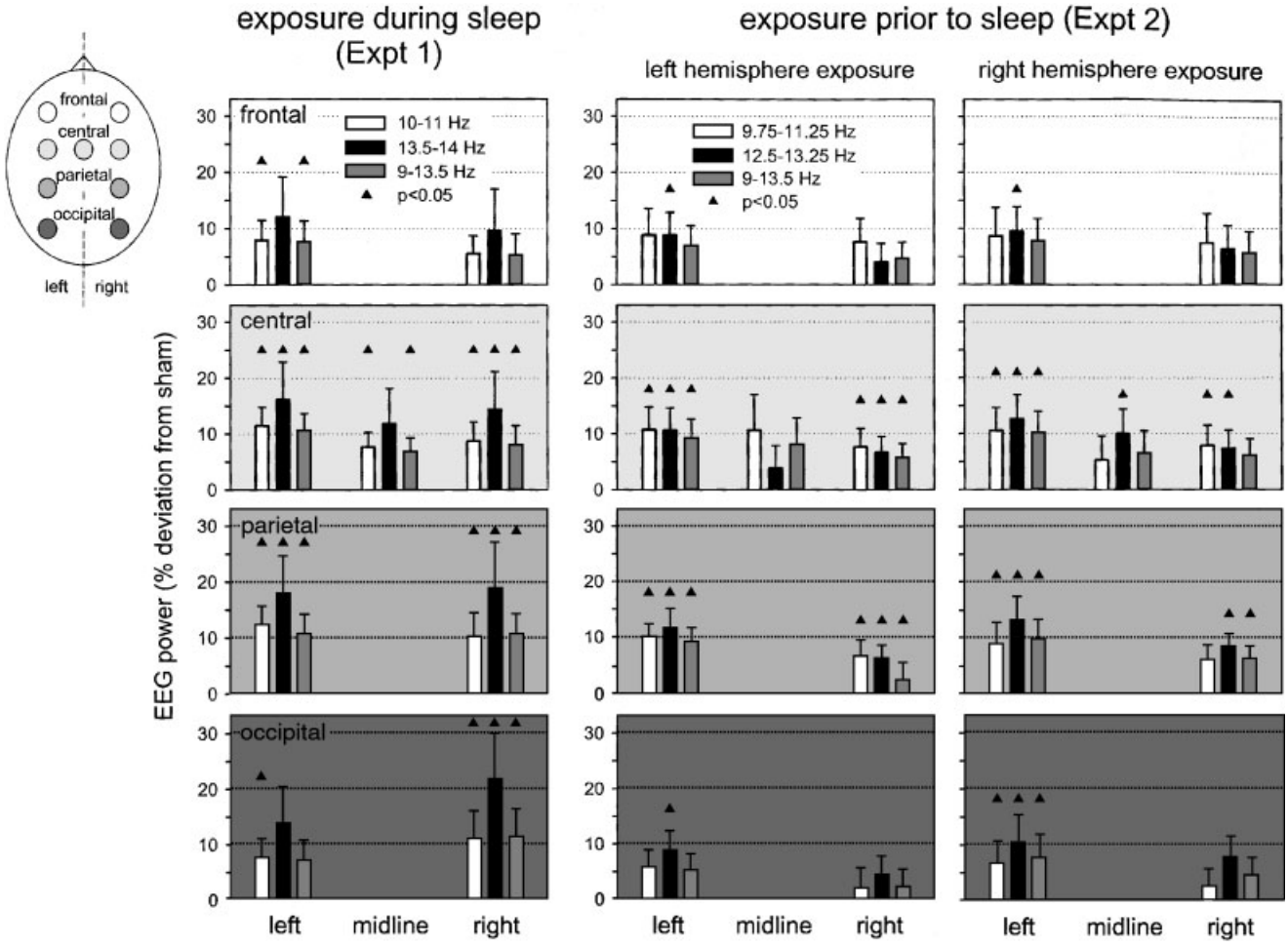

Fig. 4. Effect of RF EMF exposure on nonREM sleep EEG topography (different derivations). Mean power after RF EMF exposure expressed as a percentage of the corresponding value after sham exposure (vertical error bars represent 1 SEM). Referential derivations are illustrated (frontal F3, F4; central C3, Cz, C4; parietal P3, P4; occipital O1, O2; see pictogram). The two frequency bands exhibiting the largest changes [Borbély et al., 1999; Huber et al., 2000, Fig. 1] in each experiment and the frequency range common to both experiments are depicted (Expt 1, exposure during sleep; Expt 2, exposure prior to sleep). Filled triangles indicate significantly higher power after field exposure ($P < .05$, factor "condition" of 2 way repeated measure ANOVA performed for each derivation separately). Factor "sequence" and interaction "condition" $\times$ "sequence" were not significant.

38.2 ± 3.9; in percent of total sleep time; $P < .01$, two tailed paired t-tests). They turned their head more to the right than to the left (right: 36.5 ± 3.7; left: 24.6 ± 3.4; in percent of total sleep time; $P < .05$). No difference between field and sham exposure was observed in the time spent in any position (left, right, back), neither of the body nor in the number of position changes. Subjects placed one or both arms above their heads longer during field exposure (field: $9.9 \pm 2.9\%$ of total sleep time, sham: $2.7 \pm 1.1\%$, $P < .05$, two tailed paired t-test, $n = 14$). Only subjects with an arm displacement of at least 1 min over the entire night were considered. No order effect was observed.

Assignment of Experimental Condition (Experiment 2)

Only two out of 16 subjects assigned all three field conditions correctly. This value is not significantly different from the expected chance level of correct assignment (2.67; $P > .75$, binomial test).

DISCUSSION

Dosimetry and Energy Deposition

The exposure patterns of the two experiments are distinctly different, i.e., whole head versus unilateral

TABLE 6. Effect of RF EMF Exposure on Heart Rate

	NonREM sleep			REM sleep	Waking and stage 1	
	Sleep episode	First episode	First 30 min	Sleep episode	Sleep episode	Before sleep
Exposure during sleep (Expt 1):						
Sham	53.8 (1.7)	55.9 (1.8)	55.1 (1.7)	56.0 (1.8)	66.7 (2.0)	61.0 (2.1)
Field	53.3 (1.6)	55.0 (1.8)	54.6 (1.9)	55.6 (1.8)	66.8 (1.7)	61.3 (2.1)
Exposure prior to sleep (Expt 2):						
Sham	56.4 (1.5)		57.3 (1.5)	58.0 (1.6)	65.3 (1.7)	62.3 (2.2)
Left	56.1 (1.3)		56.0 (1.2)[a]	58.1 (1.3)	62.1 (1.3)[b]	60.2 (1.4)
Right	56.4 (1.5)		56.4 (1.5)	58.7 (1.6)	63.2 (1.6)[b]	58.2 (1.8)[b]
l + r	56.0 (1.4)		56.0 (1.3)[a]	58.1 (1.5)	62.3 (1.5)[b]	59.2 (1.6)[a]

Mean values (±SEM in parenthesis) in beats per minute are shown. Sleep episode, total sleep episode; before sleep, interval before sleep onset (first occurrence of stage 2, 3, 4, or REM sleep); l + r, average value of left and right hemispheric exposure.
[a]Indicates a trend ($P < .1$).
[b]Significant difference to sham condition ($P < .05$, two tailed paired t-test).

SAR distribution. In Expt 2 the hemispheric difference in SAR is well defined; the factor is larger than six for all investigated tissues, except for the thalamus. The differences between the two hemispheres vary in Expt 1 only by a factor of about two depending on the head posture (tilted vs. untilted). The spatial peak SAR values were the same in both studies. In Expt 1 the spatial peak was located at the top of the head, whereas in Expt 2 it was above the ear. The maximum exposure of tissues other than the brain occurred in the vertex and nose in Expt 1 and in the ear and salivary glands (submaxillary glands) in Expt 2.

In any EEG experiment conducted with RF exposure, the electrodes are primary candidates for artifacts. The following measures and studies were conducted to eliminate possible artifacts: (1) RF decoupling of amplifier and leads (see Materials and Methods section); (2) comparison of EEG recordings with RF on/off; (3) evaluation of shielding/reflection effects of the leads (reduction approx. 10%); (4) evaluation of the effect of induced currents by the leads on the spatial peak SAR (< 1% on 10 g averaged SAR). As expected, the effects of electrodes under these exposure conditions are much smaller than within the MRI environment [Chou et al., 1997; Bonmassar et al., 2002]. However, in view of the observed effects of RF EMF on the EEG, more elaborated studies are needed to assess the locally induced currents in the skin or cortex by the electrodes.

Relevance to mobile phones (both experiments). Mobile phones may expose the user to slightly higher spatial peak SAR of up to 2 W/kg [Kuster, 1997]. Furthermore, the spectral power of the 2 and 8 Hz components of the RF EMF is significantly higher for a mobile phone than for the applied signal. The exposure pattern of Expt 2 is seen as a worst case exposure scenario of mobile phones, because the exposed cortex area covers the entire area that might be exposed during usage of a mobile phone, and is strongly dependent on phone design and usage [Kuster, 2001]. The penetration depth is considerably larger than for averaged phone exposures and also slightly larger than for worst case phone exposure scenarios. However, exposure from base stations results in similar penetration depth but at lower induced field strengths.

Effects on Sleep EEG

RF EMF effects on sleep EEG have been observed in two studies under similar, but nevertheless significantly different conditions (exposure before sleep vs. exposure during sleep, unilateral exposure vs. exposure of the entire head). Under both experimental conditions nonREM sleep EEG power was increased in the 9–14 Hz range after RF EMF exposure [see Borbély et al., 1999; Huber et al., 2000].

The increase of power was similar in all derivations (Fig. 4) and may therefore represent a global effect of RF EMF exposure on sleep EEG. Even in Expt 2, in which either the right or the left hemisphere was exposed, no lateralization was observed. Power increased to a similar extent in all derivations. This result was in contradiction to our expectations, because in a previous study mechanical stimulation of the right hand had been shown to induce unilateral changes in the sleep EEG [Kattler et al., 1994].

Because the EEG effect did not depend on the side of exposure, two explanations were considered [Huber et al., 2000]: (1) the SAR ratio of about 10 to 1 (Table 3) between the exposed and nonexposed hemisphere might have been too low to induce a differential effect or a ceiling effect might have been present (i.e., the

lower field strength present at the nonexposed hemisphere may have been sufficient for a maximal effect). (2) Subcortical regions (including the thalamus) may contain the most sensitive structures to RF EMF, and their bilateral cortical projections may explain the absence of a hemispheric asymmetry. The latter explanation is supported by the high levels of the SAR in deeper brain structures including the thalamus (Table 3, Fig. 2). Because the thalamus is centrally involved in the generation of sleep spindles [Steriade et al., 1993], it represents a prime candidate for an RF EMF sensitive subcortical structure.

However, it should be noted that the sleep EEG was affected over a broad range that included the alpha range in addition to the spindle frequency range [see Borbély et al., 1999; Huber et al., 2000, Fig. 1]. Spindle oscillations are generated in the reticular nucleus of the thalamus and distributed to the cortex by thalamocortical projections [Steriade et al., 1993]. Corticothalamic feedback is a major factor in shaping and synchronizing thalamically generated spindles [Contreras et al., 1996]. High intensity electrical cortical stimulation triggered spindle oscillations, which started simultaneously in all leads [Contreras et al., 1997]. Cortical stimulation by the RF EMF may have induced changes in spindle frequency activity. However, neither the frequency of sleep spindles [location of the peak in the EEG power spectrum, Borbély et al., 1999; Huber et al., 2000] nor their pattern of occurrence was altered by exposure to RF EMF. Changes in amplitude or duration of sleep spindles cannot be detected by the current analysis. Analysis of individual spindles may be needed.

Effects on Waking EEG

We observed no consistent effect of RF EMF exposure on the waking EEG. An increase of power in the 11–11.25 Hz range in the EEG spectrum of waking and stage 1 prior to sleep onset was observed in Expt 1. Average waking EEG spectra in Expt 2 revealed a reduction of power in the 10.5–11 and 18.75–19.5 Hz frequency range. Röschke and Mann [1997] did not observe any changes in waking EEG during RF EMF exposure. The waking EEG is susceptible to artifacts. Therefore, artifact removal is important. However, statistical power was reduced, because not all subjects contributed to the data after artifact removal. The presence of sleep may be a prerequisite to reliably detect effects of RF EMF in the EEG. Expt 1 revealed that a short exposure of 15 min is sufficient for enhancing power in the sleep EEG (Fig. 3).

RF EMF exposure during sleep reduced WASO [Borbély et al., 1999]. Most subjects showed a reduction in WASO. This reduction was due to a shortening of the waking episodes during exposure. When subjects were exposed prior to sleep, WASO in the subsequent sleep episode was not affected. However, in this experiment, subjects slept in the same environment during all conditions. Therefore, there is no contradiction to our previous interpretation [Borbély et al., 1999] that RF EMF exposure counteracts the mild sleep disturbance that may have been caused by the unfamiliar experimental setup during the first experimental night in Expt 1.

Heart Rate and Heart Rate Variability

In contrast to the consistent sleep EEG effect, RF EMF exposure affected heart rate depending on the experimental setting. The observed effects were weak. RF EMF exposure prior to sleep reduced heart rate in waking and stage 1 during the whole sleep episode and in the interval from lights off to sleep onset. A trend in the same direction was observed in the first 30 min of nonREM sleep. These observations are in accordance with the data of Braune et al. [1998], who reported a decrease of heart rate after 35 min of RF EMF exposure. Heart rate was not affected when subjects were exposed during sleep. Also Mann et al. [1998] found no significant effects on heart rate when subjects were exposed during sleep. Several studies on isolated hearts showed an increase of heart rate when the exposure to electromagnetic fields induced a temperature increase [Yee et al., 1988; Pakhomov et al., 1995].

Heart rate variability as assessed by spectral analysis of consecutive RR intervals was affected during sleep in both experiments. Power around the peak in the high frequency range [0.15–0.4 Hz, Anonymous, 1996] was increased (Expt 1: 0.29–0.31 Hz; Expt 2: 0.18–0.22 Hz). Differences in the location of the high frequency peak may result from circadian factors (nighttime sleep vs. daytime sleep). In addition, in the interval prior to sleep onset spectral power of the tachogram was reduced in the low frequency range (0.10–0.11 Hz). Changes in the high frequency range are commonly attributed to vagal activity [Anonymous, 1996], whereas effects in the low frequency range are more controversial. Low frequency changes were claimed to be a marker for sympathetic modulation or a parameter that includes both sympathetic and vagal influences [Anonymous, 1996]. Mann et al. [1998] found no changes in heart rate variability in REM sleep, stage 2 and SWS when subjects were exposed during sleep. However, they did not perform a frequency bin to frequency bin comparison, which may render it difficult to observe subtle differences in the high frequency range. Altered heart rate variability was reported during nocturnal exposure to intermittent 60 Hz magnetic fields [Sastre et al., 1998, 2000]. Power in the low frequency range was reduced and in the high frequency

range increased. According to the authors, changes in thermoregulation and blood pressure control are reflected in the low frequency band, whereas changes in respiration affect the high frequency band. Due to the lack of a phase-resetting of the cardiac pacemaker, the authors hypothesized a central rather than a peripheral site of action [Sastre et al., 2000]. During nonREM sleep, an inverse relationship between EEG power in the 8–13 Hz range and the low to high frequency ratio (LF/HF) of heart rate variability was reported [Ehrhart et al., 2000]. This may point to a relationship between the effect observed in the sleep EEG and changes in heart rate variability in the present experiments.

Nevertheless, the regulation of heart rate involves many central pathways [Montano et al., 2001], and therefore conclusions about the exact mechanism of action remains speculation.

The subjective assignment of the experimental condition was not above chance level. This is consistent with the results of a recent study where it was shown that a GSM phone signal did not produce subjective symptoms [Koivisto et al., 2001]. However, due to the small sample size, statistical power is limited. Differences in arm displacement during sleep were small, on average about 30 min. It must be kept in mind that less than 60% of the subjects contributed to this finding.

CONCLUSIONS

Our studies demonstrate that exposure to RF EMF emitted by mobile phones has an effect on brain physiology. Changes in EEG power are manifested rapidly when exposure occurs during sleep (Fig. 3). They outlast exposure by at least 15 min when RF EMF is applied during waking prior to sleep [Huber et al., 2000]. Simulations of the SAR distribution within the brain support the interpretation that subcortical structures may be responsible for the observed effect on the sleep EEG.

Additional experiments are needed to identify the field characteristics (e.g., importance of modulation scheme or dose response relations) responsible for the observed EEG effects and to determine the site of interaction (exploration of different exposure locations, i.e., different parts of the head). Our findings of subtle changes in cardiac activity need to be confirmed. It is impossible to draw conclusions about the presence or absence of possible adverse effects of chronic RF EMF exposure based on the acute effects that are available.

ACKNOWLEDGMENTS

We thank Prof. Irene Tobler and Dr. Hanspeter Landolt for comments on the manuscript.

REFERENCES

Achermann P, Borbély AA. 1997. Low-frequency (< 1 Hz) oscillations in the human sleep EEG. Neuroscience 81: 213–222.

Aeschbach D, Borbély AA. 1993. All-night dynamics of the human sleep EEG. J Sleep Res 2:70–81.

Anonymous. 1996. Heart rate variability. Standards of measurement, physiological interpretation, and clinical use. Task Force of the European Society of Cardiology and the North American Society of Pacing and Electrophysiology. Eur Heart J 17:354–381.

Bonmassar G, Angelone L, Segonne F, Purdon P, Potthast A, Fischl B. 2002. Human Brain Mapping Conference. Sendai, Japan, 2002.

Borbély AA, Loepfe M, Mattmann P, Tobler I. 1983. Midazolam and triazolam: Hypnotic action and residual effects after a single bedtime dose. Arzneim-Forsch/Drug Res 33:1500–1502.

Borbély AA, Balderer G, Trachsel L, Tobler I. 1985. Effect of midazolam and sleep deprivation on day-time sleep propensity. Arzneim-Forsch/Drug Res 35:1696–1699.

Borbély AA, Huber R, Graf T, Fuchs B, Gallmann E, Achermann P. 1999. Pulsed high-frequency electromagnetic field affects human sleep and sleep electroencephalogram. Neurosci Lett 275:207–210.

Braune S, Wrocklage C, Raczek J, Gailus T, Lucking CH. 1998. Resting blood pressure increase during exposure to a radiofrequency electromagnetic field. Lancet 351:1857–1858.

Braune S, Riedel A, Schulte-Monting J, Raczek J. 2002. Influence of a radiofrequency electromagnetic field on cardiovascular and hormonal parameters of the autonomic nervous system in healthy individuals. Radiat Res 158:352–356.

Brunner DP, Münch M, Biedermann K, Huch R, Huch A, Borbély AA. 1994. Changes in sleep and sleep electroencephalogram during pregnancy. Sleep 17:576–582.

Burkhardt M, Kuster N. 2000. Appropriate modeling of the ear for compliance testing of handheld MTE with SAR safety limits at 900/1800 MHz. IEEE Trans on Microw Theory and Tech 48:1921–1934.

CENELEC. 2001. CENELEC, EN 50361, basic standard for the measurement of specific absorption rate related to human exposure to electromagnetic fields from mobile phones, Brussels, July 2001.

Chavannes NP. 2002. Local mesh refinement algorithms for enhanced modeling capabilities in the FDTD method. Zurich: ETH thesis No. 14577, 2002. p 173.

Chou C-K, Mc Dougall J-A, Chan K-W. 1997. RF heating of implanted spinal fusion stimulator during magnetic resonance imaging. IEEE Trans BME 44:367–373.

Christ A, Pokovic K, Burckhardt M, Kuster N. 1998. Sensitivity analysis of a planar antenna with respect to FDTD modelling. Atlanta, Georgia: USNC/URSI National Radio Science Meeting. 274.

Contreras D, Destexhe A, Sejnowski TJ, Steriade M. 1996. Control of spatiotemporal coherence of a thalamic oscillation by corticothalamic feedback. Science 274:771–774.

Contreras D, Destexhe A, Sejnowski TJ, Steriade M. 1997. Spatiotemporal patterns of spindle oscillations in cortex and thalamus. J Neurosci 17:1179–1196.

Driver HS, Dijk DJ, Werth E, Biedermann K, Borbély AA. 1996. Sleep and the sleep electroencephalogram across the menstrual cycle in young healthy women. J Clin Endocrinol Metab 81:728–735.

Ehrhart J, Toussaint M, Simon C, Gronfier C, Luthringer R, Brandenberger G. 2000. Alpha activity and cardiac correlates: Three types of relationships during nocturnal sleep. Clin Neurophysiol 111:940–946.

Gabriel C. 1996. Compilation of the dielectric properties of body tissues at RF and microwave frequencies. Brooks Air Force Technical Report AL/OETR-1996-0037.

Huber R, Graf T, Cote KA, Wittmann L, Gallmann E, Matter D, et al. 2000. Exposure to pulsed high-frequency electromagnetic field during waking affects human sleep EEG. NeuroReport 11:3321–3325.

Jech R, Sonka K, Ruzicka E, Nebuzelsky A, Bohm J, Juklickova M, et al. 2001. Electromagnetic field of mobile phones affects visual event related potential in patients with narcolepsy. Bioelectromagnetics 22:519–528.

Kattler H, Dijk DJ, Borbély AA. 1994. Effect of unilateral somatosensory stimulation prior to sleep on the sleep EEG in humans. J Sleep Res 3:159–164.

Koivisto M, Krause CM, Revonsuo A, Laine M, Hämäläinen H. 2000a. The effects of electromagnetic field emitted by GSM phones on working memory. NeuroReport 11:1641–1643.

Koivisto M, Revonsuo A, Krause CM, Haarala C, Laine M, Hämäläinen H. 2000b. Effects of 902 MHz electromagnetic field emitted by cellular telephones on response times in humans. NeuroReport 11:413–415.

Koivisto M, Haarala C, Krause CM, Revonsuo A, Laine M, Hamalainen H. 2001. GSM phone signal does not produce subjective symptoms. Bioelectromagnetics 22:212–215.

Krause CM, Sillanmaki L, Koivisto M, Haggqvist A, Saarela C, Revonsuo A, et al. 2000a. Effects of electromagnetic fields emitted by cellular phones on the electroencephalogram during a visual working memory task. Int J Radiat Biol 76: 1659–1667.

Krause CM, Sillanmäki L, Koivisto M, Häggqvist A, Saarela C, Revonsuo A, et al. 2000b. Effects of electromagnetic field emitted by cellular phones on the EEG during a memory task. NeuroReport 11:761–764.

Krause CM, Sillanmaki L, Koivisto M, Saarela C, Haggqvist A, Laine M, et al. 2000c. The effects of memory load on event-related EEG desynchronization and synchronization. Clin Neurophysiol 111:2071–2078.

Kuster N. 1997. Mobile communications safety. London: Chapman & Hall.

Kuster N. 2001. Latest progress in experimental dosimetry for human exposure evaluations and for characterization hand optimization of exposure setups used in biological experiments. Paris: CADAS, Academie des Sciences.

Kuster N, Kästle R, Schmid T. 1997. Dosimetric evaluation of handheld mobile communications equipment with known precision. IEICE Trans Commun E80-B:645–651.

Landolt HP, Dijk DJ, Gaus SE, Borbély AA. 1995a. Caffeine reduces low frequency delta activity in the human sleep EEG. Neuropsychopharmacology 12:229–238.

Landolt HP, Werth E, Borbély AA, Dijk DJ. 1995b. Caffeine intake (200 mg) in the morning affects human sleep and EEG power spectra at night. Brain Res 675:67–74.

Mann K, Röschke J. 1996. Effects of pulsed high-frequency electromagnetic fields on human sleep. Neuropsychobiology 33:41–47.

Mann K, Röschke J, Connemann B, Beta H. 1998. No effects of pulsed high frequency electromagnetic fields on heart rate variability during human sleep. Neuropsychobiology 38: 251–256.

McCormick DA, Bal T. 1997. Sleep and arousal: Thalamocortical mechanisms. Ann Rev Neurosci 20:185–215.

Montano N, Cogliati C, Dias da Silva VJ, Gnecchi-Ruscone T, Malliani A. 2001. Sympathetic rhythms and cardiovascular oscillations. Auton Neurosci 90:29–34.

NIST TN1297. 1994. Guidelines for evaluating and expressing the uncertainty of NIST measurement results. Gaithersburg, MD: National Institute of Standards and Technology.

Pakhomov AG, Dubovick BV, Degtyariov IG, Pronkevich AN. 1995. Microwave influence on the isolated heart function: I. Effect of modulation. Bioelectromagnetics 16:241–249.

Preece AW, Iwi G, Davies-Smith A, Wesnes K, Butler S, Lim E, et al. 1999. Effect of a 915-MHz simulated mobile phone signal on cognitive function in man. Int J Radiat Biol 75:447–456.

Rechtschaffen A, Kales A. 1968. A manual of standardized terminology, techniques and scoring system for sleep stages of human subjects. Bethesda, Maryland: National Institutes of Health.

Roth C, Landolt HP, Achermann P, Teuscher A, Borbély AA. 1998. Human versus porcine insulin in patients with insulin-dependent diabetes mellitus: Differences in sleep and the sleep EEG during nearnormoglycemia. Sleep 21:92–100.

Röschke J, Mann K. 1997. No short-term effects of digital mobile radio telephone on the awake human electroencephalogram. Bioelectromagnetics 18:172–176.

Sastre A, Cook MR, Graham C. 1998. Nocturnal exposure to intermittent 60 Hz magnetic fields alters human cardiac rhythm. Bioelectromagnetics 19:98–106.

Sastre A, Graham C, Cook MR. 2000. Brain frequency magnetic fields alter cardiac autonomic control mechanisms. Clin Neurophysiol 111:1942–1948.

Schmid T, Egger O, Kuster N. 1996. Automated E-field scanning system for dosimetric assessments. IEEE Trans on Microw Theory and Tech 44:105–113.

Schüller M, Streckert J, Bitz A, Menzel K, Eicher B. 2000. Proposal for generic GSM test signal. Proc 22nd BEMS Annual Meeting, pp 122–123.

Steriade M, McCormick DA, Sejnowski TJ. 1993. Thalamocortical oscillations in the sleeping and aroused brain. Science 262: 679–685.

Steriade M, Contreras D, Amzica F. 1994. Synchronized sleep oscillations and their paroxysmal developments. Trends Neurosci 17:199–208.

Tisserand DJ, Bosma H, Van Boxtel MP, Jolles J. 2001. Head size and cognitive ability in nondemented older adults are related. Neurology 56:969–971.

Wagner P, Röschke J, Mann K, Hiller W, Frank C. 1998. Human sleep under the influence of pulsed radiofrequency electromagnetic fields—A polysomnographic study using standardized conditions. Bioelectromagnetics 19:199–202.

Wagner P, Röschke J, Mann K, Fell J, Hiller W, Frank C, et al. 2000. Human sleep EEG under the influence of pulsed frequency electromagnetic fields. Neuropsychobiology 42:207–212.

Yee KC, Chou CK, Guy AW. 1988. Influence of microwaves on the beating rate of isolated rat hearts. Bioelectromagnetics 9:175–181.